

Optical flow measurement of human walking

Qingwen Liu, Okuary Osechas, and Jason H. Rife

Tufts University

>> Accepted Article <<

CITATION:

Q. Liu, O. Osechas, and J. Rife (2012). Optical flow measurement of human walking. Proc. IEEE/ION Position, Location, and Navigation Symposium (PLANS 2012), Myrtle Beach, SC. DOI: 10.1109/PLANS.2012.6236926.

CORRESPONDING AUTHOR:

Jason Rife

jason.rife@tufts.edu

COPYRIGHT:

© 2012 IEEE. Personal use of this material is permitted. Permission from IEEE must be obtained for all other uses, in any current or future media, including reprinting/republishing this material for advertising or promotional purposes, creating new collective works, for resale or redistribution to servers or lists, or reuse of any copyrighted component of this work in other works.

Optical Flow Measurement of Human Walking

Qingwen Liu, Okuary Osechas, and Jason Rife

Tufts University
Medford, MA

{qingwen.liu, okuary.osechas, jason.rife}@tufts.edu

Abstract—This paper presents a method for using optical flow measurements to estimate stride length for pedestrian navigation applications. Optical flow sensors, such as the detectors used in an optical computer mouse, measure the velocity of visual features traversing an imaging array. We consider the case in which the optical flow sensor is attached to the leg of a pedestrian and used to infer distance traveled. In this configuration, optical flow data are a projection of the velocity and angular velocity of the leg to which the sensor is attached; a dynamic motion model is needed to estimate leg states and to infer stride length from the optical flow data. In this paper, we consider a very simple dynamic walking model, called the Spring Loaded Inverted Pendulum (SLIP) model. In a hardware-based trial, the basic SLIP model estimated stride length with 10% error. We anticipate that refinements to the basic SLIP model will enable more accurate stride-length estimation in the future.

Keywords—Optical Flow, Pedestrian Navigation

I. INTRODUCTION

In this paper, we propose a novel methodology for pedestrian navigation that combines camera-based optical flow measurements with a dynamic walking model, called the Spring-Loaded Inverted Pendulum (SLIP) model. An optimization strategy is used to match the experimental data to simulation data, giving an estimate of the stride length.

Pedestrian navigation is of particular interest in indoor environments. Despite its wide coverage outdoors, Global Positioning System (GPS) signals are not available indoors, and degrade significantly in deep city canyons. This has led researchers to focus on developing alternative navigation methods for pedestrian applications in indoors and other GPS-denied environments.

Many emerging applications demand high-accuracy, indoor navigation for pedestrians. Emergency responders, for example, would benefit from high accuracy indoor positioning to aid in quickly locating their destinations in unfamiliar buildings or in emergency escape from buildings, especially when visibility is poor. Consumer applications are also of interest, such as guidance in an unfamiliar museum or shopping mall. Such systems would provide particularly high benefits for the vision-impaired [1].

Given the potentially large market for pedestrian navigation, many technologies have been proposed. Most proposed strategies fall into three categories: beacon-based, inertial-based and vision-based navigation.

Beacon-based methods rely on sensors such as infrared, ultrasound or Ultra-Wideband Impulse Radio (UWB-IR) sensors [2]-[3][4] and even Wi-Fi hotspots [5]. Beacon-based methods are based on principles similar to those underlying GPS navigation, measuring distances from a receiver to transmitters with known locations. These strategies are relatively accurate but require specialized infrastructure.

Inertial-based methods oftentimes make use of low-cost Inertial Measurement Unit (IMU) to collect acceleration data [6]. The accuracy of these dead-reckoning technologies depends largely on the quality of the IMU itself and that of the stride length estimation function.

Among the vision-based methods, numerous techniques have been proposed; most vision-based navigation algorithms rely on feature tracking [7]. Methods that identify and track features typically employ high resolution images. As image resolution increases, more power must be supplied to the imaging array and more computation is required to process the full image.

This paper considers the use of Optical Flow (OF) sensors for pedestrian navigation. OF sensors are imaging arrays that sense motion in two-dimensions, lateral to the imaging array. Optical flow measurements may be obtained from conventional video cameras or from more compact sensors, similar to those designed for use in an optical computer mouse (see Fig. 1). Recently, compact, low-power optical flow sensors have been custom-built for use in small Unmanned Aerial Vehicles [8].

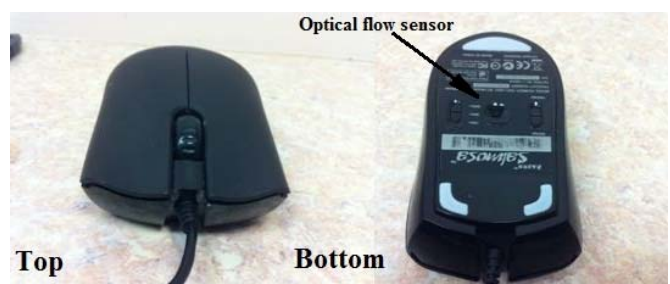


Fig. 1. Optical Flow Sensor for Computer Mouse

OF sensing addresses some of the shortcomings in previously described methods. Specifically, OF sensing requires lower power and processing requirements than typical vision-based methods, because computing optical flow requires

only a very small number of image-array pixels. Furthermore, OF overcomes one of the limitations of IMU-based navigation in that OF dead-reckoning errors are believed to accumulate more slowly than IMU dead-reckoning errors. This occurs because errors that affect optical flow (velocity measurement) need only be integrated once to obtain displacement, and not twice as is the case for accelerometer measurements.

A complication of inferring displacement from OF data is that OF depends on both the velocity and angular velocity of the imaging array. In this paper, we study pedestrian navigation using a single OF sensor; hence, a dynamic model is needed to relate the OF signal to the combined velocities and angular velocities that generated the signal. For this purpose, we propose using one of the simplest walking models that has been developed for the study of human gait: the SLIP model. Specifically, the SLIP model is used to infer leg motion and, thereby, to relate optical flow measurements to stride length.

The remainder of the paper is organized as follows. First we present general background information regarding OF algorithms and the SLIP walking model. In the subsequent section we discuss a specific system configuration for OF-based pedestrian navigation. The results of a hardware-based verification of the method are discussed in the penultimate section. A brief summary concludes the paper.

II. BACKGROUND

A. Optical Flow

OF is caused by the motion of features in the image plane due to the relative movement between an observer and the surrounding environment. In the animal kingdom, intelligent creatures such as bees depend on their built-in optical flow field observation system for obstacle avoidance and route recognition [9]. Human beings are also thought to depend on optical flow for navigation.

Based on natural inspiration, a large number of OF algorithms have been proposed in the field of computer vision. The idea of optical flow was first introduced in the 1950s, and research has focused on developing a variety of algorithms to determine OF fields. Currently, three major categories of OF algorithms can be identified: gradient-based, correlation-based and spatiotemporal-based method. Typical optical flow algorithms extract only two components of motion: horizontal velocity along each axis of pixel array (in units of pixels per second). Extensions that infer angular velocity or three-dimensional velocity are possible in some cases for applications using large imaging arrays.

In this paper, we will focus on algorithms appropriate for compact, light-weight, low-power sensors capable of making only two-dimensional optical flow measurements. In particular, we will assume optical flow measurements are made using an imaging array attached to the lower section of the human leg and pointed along the axis between the knee and the ankle. Stride length, meaning the distance traveled by a pedestrian between successive heel strikes by the same foot, cannot be directly inferred from a ground-looking optical flow sensor mounted on the leg, due to the imaging array's variable

distance from the terrain and its unknown angular velocity. One means of recovering stride length from such optical flow measurements is to run a dynamic walking model in real-time, and to adjust model parameters until the simulated optical flow matches actual sensor measurements.

B. Human Walking Model

Understanding human walking patterns is still an open topic discussed in literature. Many different models have been proposed, including kinematic, dynamic and energy-related models. Some researchers make certain assumptions and build robots mimicking the behavior of human walking. Two famous models, the passive walker [10] and the SLIP model [11], are well-studied.

We focus on the SLIP model because it is simple and straightforward, an important consideration in reducing computational complexity. The SLIP model is well-studied and it can be tuned to represent both walking and running. Robots based on SLIP models have been constructed in the past 10 years, and they have succeeded in mimicking the basic behavior of human walking. A particular benefit of the SLIP model is that it can describe dynamic walking without any need to identify models for human muscle or for the control commands sent to those muscles.

III. METHODS

A. System Configuration

Estimating stride length is the main objective of the methodology presented in this paper. The methodology is intended for real-time implementation using a compact optical flow sensor [12] complemented by a microprocessor that integrates the dynamic walking simulation. For development purposes, however, the research described in this paper used an off the shelf camera, from which data were processed offline on a desktop computer. Video data from the camera are processed and compared to the SLIP simulation as shown in the algorithm block diagram (Fig. 2).

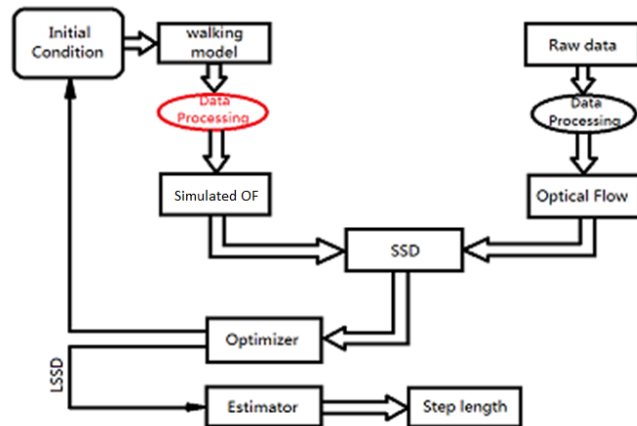


Fig. 2. System Configuration

In our methodology, stride-length is estimated by an algorithm that compares sensor measurements to simulated data. OF sensor measurements are obtained by processing a series of video frames. Simulated OF data are generated from a simulation based on the SLIP model. Both the measurement branch (that converts raw data to optical flow measurement) and the simulation branch (that converts the walking model into simulated OF) are clearly visible in the block diagram. The algorithm seeks to match the measured and simulated OF data by comparing their differences using a sum of squared differences (SSD). An optimizer attempts to minimize the SSD by adjusting the initial conditions and control parameters for the simulation. When the SSD algorithm converges to obtain the least sum of squared differences (LSSD), the corresponding stride length is selected as the best estimate of the actual stride length. It is assumed that the SSD calculation is run on batch mode over an extended series of data, consisting of at least one stride and possibly many strides.

B. Optical Flow Measurement

This section describes the algorithms we used to obtain OF measurements from imaging array data. As described in the previous section, optical flow measurements are compared to simulated optical flow (generated from a SLIP model) in order to infer stride length.

OF is defined as a vector field describing the motion of features across the imaging array, in units of pixels/second. The OF vector \mathbf{f} consists of two components, the pixel velocities u and v , each associated with one of the imaging array's orthogonal coordinate directions.

$$\mathbf{f} = \begin{bmatrix} u \\ v \end{bmatrix} \quad (1)$$

In special cases, OF is the same at all pixels across the imaging array; for instance, if the imaging array moves in a plane parallel to a highly textured, stationary, planar surface, then the OF field is uniform at all points in the imaging array. In more general scenarios, the OF field is not uniform. For instance, if an imaging array moves toward a planar surface, then OF vectors point outwards from the image center (much as the tracks of stars appear to move radially outward during a "jump to hyperspace" in a certain science fiction movies.)

In this paper, OF measurements were computed using the algorithm described in [12]. Rather than compute the full OF field across the image, this algorithm only computes the 2D OF vector at the image center. Optical flow \mathbf{f} is computed by solving the following matrix equation.

$$\mathbf{A} \mathbf{f} = \mathbf{b} \quad (2)$$

Here the \mathbf{A} and \mathbf{b} matrices are expressed in terms of the spatial and temporal derivatives of a video sequence obtained from the imaging array. The notation $I(x,y,t)$ is used to refer to each intensity image from the video sequence, where pixel locations are identified by the pair of integer pixel coordinates x and y and where each sample time is denoted by the continuous time variable t . Discretized spatial derivatives (dI/dx and dI/dy) and the temporal derivative (dI/dt) of the image sequence are defined as follows.

$$\begin{aligned} \frac{dI}{dx} &= \frac{I(x + \Delta x_{ref}, y, t) - I(x - \Delta x_{ref}, y, t)}{2\Delta x_{ref}} \\ \frac{dI}{dy} &= \frac{I(x, y + \Delta y_{ref}, t) - I(x, y - \Delta y_{ref}, t)}{2\Delta y_{ref}} \\ \frac{dI}{dt} &= \frac{I(x, y, t - \Delta t) - I(x, y, t)}{\Delta t} \end{aligned} \quad (3)$$

Here Δx_{ref} and Δy_{ref} are integer parameters (both with values of 20 pixels in our implementation of the algorithm), and Δt is the time interval between sampled images (approximately 0.06 sec for our system).

OF can be related to spatial and temporal gradients by assuming the image intensity is a conserved quantity [13]-[15], as in the following definitions of \mathbf{A} and \mathbf{b} .

$$\mathbf{A} = \begin{bmatrix} \sum_{x,y} \left(\Psi(x,y) \left(\frac{dI}{dx} \right)^2 \right) & \sum_{x,y} \left(\Psi(x,y) \frac{dI}{dx} \frac{dI}{dy} \right) \\ \sum_{x,y} \left(\Psi(x,y) \frac{dI}{dx} \frac{dI}{dy} \right) & \sum_{x,y} \left(\Psi(x,y) \left(\frac{dI}{dy} \right)^2 \right) \end{bmatrix} \quad (4)$$

$$\mathbf{b} = \begin{bmatrix} \sum_{x,y} \left(\Psi(x,y) \frac{dI}{dt} \frac{dI}{dx} \right) \\ \sum_{x,y} \left(\Psi(x,y) \frac{dI}{dt} \frac{dI}{dy} \right) \end{bmatrix} \quad (5)$$

These matrices compute the OF value near the image center as a weighted average over many pixels, where the weighting function Ψ is a Gaussian with its maximum value at the image center, where (x,y) is $(0,0)$.

$$\Psi(x,y) = e^{-2.772(x^2+y^2)/p^2} \quad (6)$$

The width parameter p defines the spatial extent of the Gaussian weighting filter, with pixel weights falling off to 6% of their peak values at a radius of p . In this work, p was set to a value of 120 pixels.

An important limitation of OF is that it cannot be computed when observing a monochromatic surface (e.g., a white wall). The above OF formulation, based on (4) and (5), addresses the monochromatic-surface problem by introducing a weighting based on pixel gradient. All terms in the first line of (2) are scaled by the image gradient in one direction (by dI/dx); all terms in the second line of (2) are scaled by the orthogonal image gradient (by dI/dy). Regions of the image with low texture (e.g., regions of uniform intensity) have very small gradients and, hence, have low weights.

C. SLIP Model

This section describes the SLIP motion model used to simulate the trajectory of the OF sensor. In the estimation process, the input parameters to this model are iteratively adjusted until simulated OF data closely match the OF measurements described in the previous section.

The SLIP model describes the motion of the hip during walking and running. The model is highly simplified in that all body mass is lumped at a single point (i.e., at the hip). Accordingly, the hip is also referred to as the center of mass G , as shown in Fig. 3. It should be noted that this placement of the center of mass of the SLIP model at the hip is an approximation (as the center of mass of most humans does not fall precisely at the hip). The SLIP model assigns no mass to the legs; nor is the leg geometry explicitly modeled. Rather the leg is simply represented as a spring-like force that acts on the hip, so long as the foot is in contact with the ground.

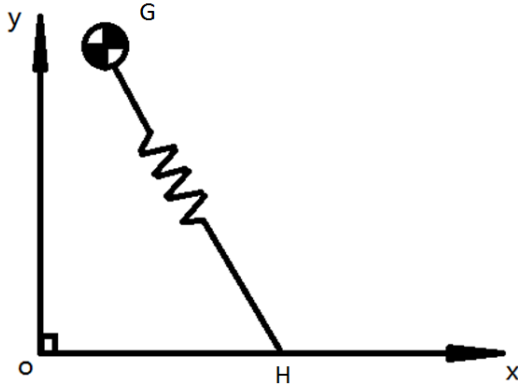


Fig. 3. SLIP Model Visualized at One Instant

The particular form of the SLIP model used in this research, assumes that the leg force offsets gravity and provides an additional spring force \mathbf{F}_s as described in the following equation.

$$m \ddot{\mathbf{x}}_G = \mathbf{F}_s \quad (7)$$

Here m is the lumped mass of the pedestrian and \mathbf{x}_G is the position vector describing the location of the hip in the sagittal plane. Forces exerted by muscles, tendons and bones within the leg are modeled with a spring force \mathbf{F}_s . The spring force acts between the hip and the heel contact point H . If the position vector to the heel is defined to be \mathbf{x}_H , the spring equation has the following form, where L_{ref} is the maximum reference length of the spring.

$$\mathbf{F}_s = \begin{cases} k (L_{ref} - L) \frac{\mathbf{x}_G - \mathbf{x}_H}{L}, & L \leq L_{ref} \\ 0, & \text{otherwise} \end{cases} \quad (8)$$

In this equation, the length L is defined

$$L = \|\mathbf{x}_G - \mathbf{x}_H\|, \quad (9)$$

and the reference length L_{ref} is equal to the total leg length, including the hip-to-knee (or thigh) length L_{th} and the knee-to-heel (or shank) length L_{sh} :

$$L_{ref} = L_{th} + L_{sh}. \quad (10)$$

This model implicitly assumes that either one leg or the other is always in contact with the ground. The first leg is lifted off the ground (an event called *toe off*) at the same instant that the second leg contacts the ground (an event called *heel strike*). This simplified model does not specifically simulate *double stance* (in which both legs are in contact with the ground simultaneously) or *flight* (in which neither leg is in contact with the ground). Because flight is not permitted in our simulations, it is assumed that the pedestrian shifts from heel contact to toe contact if the length L exceeds L_{ref} .

The SLIP model implemented in this work makes no distinction between left and right feet. Step transitions between left foot and right foot contact are assumed to occur whenever the hip is descending ($\mathbf{v}_G \cdot \hat{\mathbf{y}}_w < 0$) and the hip passes through a critical height h_{crit} . The critical height strongly influences gait evolution. The critical height is set by assuming a leg angle (relative to the vertical) at the moment of heel strike; this control parameter is labeled δ_{hs} .

$$h_{crit} = (L_{th} + L_{sh}) \cos \delta_{hs}, \quad (11)$$

This equation assumes the leg is fully extended at the moment of heel strike.

At the moment when heel strike occurs, the heel contact point is updated as weight transitions to a new foot. An integer index k is used to refer to each of these transitions. The heel contact point at the time of the transition is set by the following equation.

$$\mathbf{x}_H(k) = \mathbf{x}_G + h_{crit} \begin{bmatrix} \tan \delta_{hs} \\ -1 \end{bmatrix} \quad (12)$$

It is assumed that the odd indices k refer to foot placement involving the foot on which the OF sensor is placed. Even indices correspond to the opposite foot.

D. Leg Kinematics Model

Because SLIP captures only the dynamics of the lumped mass at the hip, it does not explicitly predict leg motion, as might a more detailed passive walker model [16]. As such, leg kinematics must be inferred from the hip states computed by the SLIP model. The notion of algebraically inferring the states of a complex model (also called an anchor) from a simple dynamic model (also called a template) has been studied extensively in the fields of comparative biology and biomimetic robotics [17].

In our implementation, the leg model consists of three rigid links, an upper leg (thigh), a lower leg (shank), and a foot. All three segments are illustrated in Fig. 4. The thigh extends a length L_{th} from the hip G to the knee K . The shank extends a length L_{sh} from the knee K to the heel H . The foot extends a length L_{fi} from the heel H to the toe T (which might more accurately be labeled the ball of the foot). It is assumed that the heel remains on the ground as long as the hip to heel-contact-point distance L does not exceed the combined length of the thigh and shank; when this limit is exceeded, the foot is assumed to rotate about the toe contact point T to allow the hip to travel farther (and for L to continue to increase).

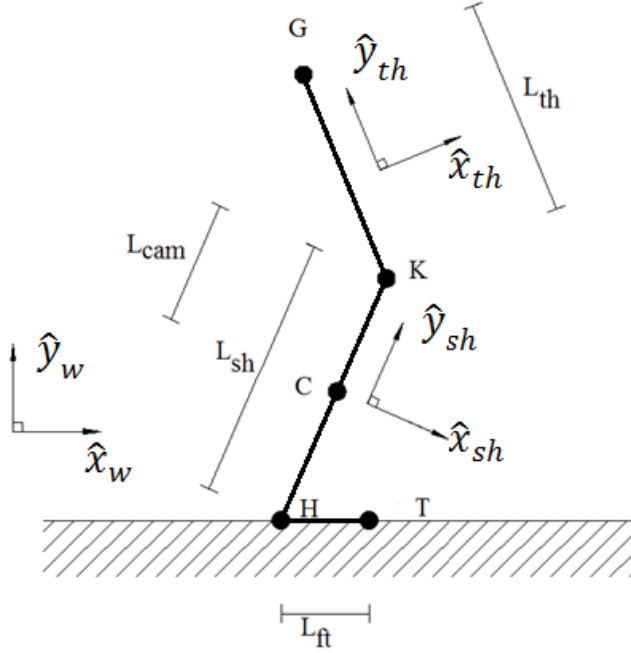


Fig. 4. Leg Geometry

The focal point of the optical flow sensor (e.g., the camera) is positioned along the shank at a distance L_{cam} relative to the knee. It is assumed that the camera is pointing along and rotates with the shank reference frame (sh subscript). Reference frames attached to the thigh (th subscript) and to the world frame (w subscript) are also illustrated in Fig. 4. Unit vectors for each frame are indicated as the vectors \hat{x} and \hat{y} , followed by appropriate subscripts to indicate their frame.

The position of the hip is known from simulation; so the position of the camera can be computed if the coordinate system of the shank and thigh are known.

$$\mathbf{x}_C = \mathbf{x}_G - L_{th}\hat{\mathbf{y}}_{th} - L_{cam}\hat{\mathbf{y}}_{sh} \quad (13)$$

The point on the ground at the center of the camera optical axis is identified by the following equation, assuming the optical axis is aligned with ground. Here D is distance from camera focal point to the point P where the camera optical axis intersects the ground plane.

$$\mathbf{x}_P = \mathbf{x}_G - L_{th}\hat{\mathbf{y}}_{th} - (L_{cam} + D)\hat{\mathbf{y}}_{sh} \quad (14)$$

Optical flow measurements are scaled by the distance D , which can be determined by dotting the above equation with the vertical unit vector $\hat{\mathbf{y}}_w$ and assuming that the height of the ground plane is zero.

$$D = \frac{\mathbf{x}_G \cdot \hat{\mathbf{y}}_w - L_{th}\hat{\mathbf{y}}_{th} \cdot \hat{\mathbf{y}}_w}{\hat{\mathbf{y}}_{sh} \cdot \hat{\mathbf{y}}_w} - L_{cam} \quad (15)$$

Optical flow depends directly on the OF sensor's velocity, which is:

$$\mathbf{v}_C = \mathbf{v}_G + \omega_{th}L_{th}\hat{\mathbf{x}}_{th} + \omega_{sh}L_{cam}\hat{\mathbf{x}}_{sh}. \quad (16)$$

More specifically, OF measurements depends only on the component of this velocity perpendicular to the optical axis (e.g., perpendicular to $\hat{\mathbf{y}}_{sh}$). Hence, the OF model will depend only on the component of velocity normal to the shank (e.g., on $\mathbf{v}_C \cdot \hat{\mathbf{x}}_{sh}$).

Optical flow is also sensitive to shank rotation. The angular velocity, as well as the thigh and shank pointing vectors, must be treated separately for each of three configurations. Namely, different equations are needed to solve for the angular velocity and pointing vectors when (1) the heel contacts the ground, (2) the toe contacts the ground, and (3) the foot does not contact the ground.

In the first configuration, when the heel is in contact with the ground, the thigh and shank rotation rates may be computed by solving the following equation for two angular velocity terms, noting that the heel velocity \mathbf{v}_H is zero and that the hip velocity \mathbf{v}_G is known from the SLIP simulation.

$$\mathbf{v}_H = \mathbf{0} = \mathbf{v}_G + \omega_{th}L_{th}\hat{\mathbf{x}}_{th} + \omega_{sh}L_{sh}\hat{\mathbf{x}}_{sh}. \quad (17)$$

In this configuration (heel in contact with the ground), the unit vectors $\hat{\mathbf{y}}_{th}$ and $\hat{\mathbf{y}}_{sh}$ are computed from the following equation.

$$\mathbf{x}_H(k) - \mathbf{x}_G = -L_{th}\hat{\mathbf{y}}_{th} - L_{sh}\hat{\mathbf{y}}_{sh} \quad (18)$$

Here $\mathbf{x}_H(k)$ is the current heel position, which is stationary during step k (e.g., during stance). In order to compute the four unknown components of the two unit vectors in (18), it is necessary to invoke two additional constraint equations (namely, that the vectors are of unit length) in order to match the number of equations to the number of unknowns. The perpendicular unit vectors, $\hat{\mathbf{x}}_{th}$ and $\hat{\mathbf{x}}_{sh}$, can be obtained by a cross product of the computed $\hat{\mathbf{y}}$ vectors with the vector pointing out of the plane.

In the second configuration, when only the toe touches the ground, angular velocities are computed with the following equation

$$\mathbf{v}_T = \mathbf{0} = \mathbf{v}_G + \omega_{th}(L_{th} + L_{sh})\hat{\mathbf{x}}_{th} + \omega_{ft}L_{ft}\hat{\mathbf{y}}_{sh}, \quad (19)$$

where it is assumed the thigh and shank rotate together such that their coordinate systems are aligned and their angular velocities are equal ($\omega_{th} = \omega_{sh}$). The unit vectors for each frame can be computed with a modified version of (18), where the contact point occurs at the toe:

$$\mathbf{x}_T(k) - \mathbf{x}_G = -(L_{th} + L_{sh})\hat{\mathbf{y}}_{th} + L_{ft}\hat{\mathbf{x}}_{ft} \quad (20)$$

with

$$\mathbf{x}_T(k) = \mathbf{x}_H(k) + L_{ft}\mathbf{x}_w. \quad (21)$$

Additional assumptions must be made to compute the angular rotation rates during swing, when the foot is not in contact with the ground, since the SLIP model provides no information about the leg during swing. In our model, we characterize swing by considering the *nominal* pointing vector, which describes the unit vector $\hat{\mathbf{u}}_{nom}$ from the hip to the heel. As a rough heuristic, we assume that this nominal pointing vector rotates with a constant angular velocity. This nominal angular velocity ω_{nom} transforms $\hat{\mathbf{u}}_{nom}$ between its starting direction at the beginning of swing (at time $t_{crit,k}$) and its final direction at the end of swing (at time $t_{crit,k+1}$).

$$\omega_{nom} = \frac{\arccos(\hat{\mathbf{u}}_{nom}(t_{crit,k}) \cdot \hat{\mathbf{u}}_{nom}(t_{crit,k+1}))}{\Delta t_k} \quad (22)$$

Here the total length of the k -th swing phase is Δt_k .

$$\Delta t_k = t_{crit,k+1} - t_{crit,k} \quad (23)$$

The pointing vector at the beginning and end of swing can be computed from the known heel locations at each time using the following equation.

$$\hat{\mathbf{u}}_{nom} = \frac{\mathbf{x}_H - \mathbf{x}_G}{\|\mathbf{x}_H - \mathbf{x}_G\|} \quad (24)$$

The hip-to-heel pointing vector at intermediate times has the following form, where $\mathbf{R}(\theta)$ is a 2D rotation matrix through the angle θ .

$$\hat{\mathbf{u}}_{nom}(t) = \mathbf{R}\left(\omega_{nom}\left(\frac{t - t_{crit,k}}{\Delta t_k}\right)\right) \hat{\mathbf{u}}_{nom}(t_{crit,k}) \quad (25)$$

The thigh angle is assumed to change somewhat faster than ω_{nom} during swing, which results in knee deflection. The assumed perturbation of the knee angle $\delta\theta_{th}$ from the nominal leg direction is modeled as a parabolic function of time t .

$$\delta\theta_{th} = a(1 - \tilde{t}^2) + b(\tilde{t} - \tilde{t}^2) \quad (26)$$

Given the normalized time coordinate \tilde{t} is defined on the range between zero and one as

$$\tilde{t} = \frac{t - t_{crit,k}}{t_{crit,k+1} - t_{crit,k}}, \quad (27)$$

the parameter a is the initial thigh perturbation angle, and the parameter b is related to the maximum thigh perturbation angle a_{max} (which was set equal to a scalar multiple of a in this paper). To ensure the desired maximum angle a_{max} is reached,

$$b = 2(a_{max} - a) \left(1 + \sqrt{1 + \left(\frac{a_{max}}{a} - 1\right)^{-1}} \right). \quad (28)$$

Taking the derivative of (26), the perturbed angular velocity of the thigh is

$$\delta\omega_{th} = \left(a(2\tilde{t}) + b(1 - 2\tilde{t}) \right) \frac{1}{\Delta t_k}. \quad (29)$$

Noting that the heel lies along the vector $\hat{\mathbf{u}}_{nom}$, which points from the hip to the heel, the angular velocity of the shank ω_{sh} can be computed to be:

$$\omega_{sh} = \omega_{nom} - \frac{L_{th} \cos(\delta\theta_{th})}{L_{sh} \sqrt{1 - L_{th}^2 \sin^2(\delta\theta_{th}) / L_{sh}^2}} \delta\omega_{th}. \quad (30)$$

E. Optical Flow Simulation

Simulated optical flow measurements are computed from projective geometry as described by [8]. The equation that simulates the OF measurement \mathbf{f} is:

$$\mathbf{f}_{sim} = -f \left(\frac{\mathbf{v}_c \cdot \hat{\mathbf{x}}_{sh}}{D} + \omega_{sh} \right) \quad (31)$$

This equation depends on the sensor focal length f , on the lateral sensor velocity $\mathbf{v}_c \cdot \hat{\mathbf{x}}_{sh}$, on the distance D from the focal point to the ground plane, and on the angular velocity of the shank ω_{sh} .

IV. VERIFICATION

A preliminary demonstration was conducted to verify our concept for OF-based pedestrian navigation. Given the approximate nature of the SLIP model, the main goal of the verification study was to quantify how well the SLIP model describes bipedal walking and how accurately an estimator based on SLIP infers stride length.

A. Test Configuration

Concept verification was conducted indoors. A five-meter long track was configured for testing. In order to gain full information from video data, the test track was covered in newspaper (see Fig. 5). The newspaper provided high contrast patterns that enhanced the quality of OF measurements. Because the newspaper suppressed optical-flow measurement noise, the factor most limiting performance was expected to be the SLIP model. Markers were placed on the ground to provide ‘‘truth data’’ to which to compare our stride length estimates. The test engineer attempted to step on each marker, so that stride length was predetermined. Only straight line walking was considered.

To simplify device design and provide full access to data during testing, we employed a conventional video camera in place of a more compact, low-power OF sensor. The camera was attached at the outer side of knee, pointing along the length of the shank, such that the camera optical axis was approximately vertical when the test engineer was standing upright (see Fig. 6). Video frames were recorded continuously and post-processed on a separate computer.



Fig. 5. Test Track



Fig. 6. Conventional Video Camera Used for Concept Verification

B. Test Results

The methodology described in Section III was applied to OF data collected on the test track. The parameters describing the motion model are summarized in Table 1 below. Length parameters were measured with a ruler. The mass parameter was measured with a scale. The leg stiffness parameter k was inferred as an estimated state for this trial, but would be fixed as a static parameter for later trials.

TABLE 1. PHYSICAL PARAMETERS FOR SLIP MODEL

Parameter	Value
Thigh Length L_{th}	0.5 m
Shank Length L_{sh}	0.6 m
Foot Length L_{ft}	0.2 m
Body Mass m	50 kg
Leg Stiffness k	$1.8 \cdot 10^4$ N/m

The optimization routine identified a best match between the simulation and the optical-flow measurements for the case when the initial condition (at the instant of heel strike for the

leg with the OF sensor) was $\mathbf{v}_G = [1.6 \ -0.5]^T$ m/sec. The best match occurred when the control parameter δ_{hs} , which describes leg angle from vertical at the moment of heel strike, was 10.4° .

Only a single trial was conducted. For this trial, the true value of the stride length was 1.2 m. The stride length estimated using the SLIP model was 1.06 m. Thus, the estimation error was approximately 10%.

The OF measurements for the trial are illustrated in Fig. 7. The corresponding simulated OF data for the best-match simulation parameters are shown in Fig. 8. It should be noted that the focal length f was not explicitly considered in estimating the simulated OF. Also, because the transition between one foot and the other was not actually instantaneous, as assumed in the SLIP model, we decide to introduce a weighting function in computing the SSD, counting all points in the swing phase (when the heel was not in contact with the ground) with five times the weight of points in the stance phase (when the heel was in contact with the ground).

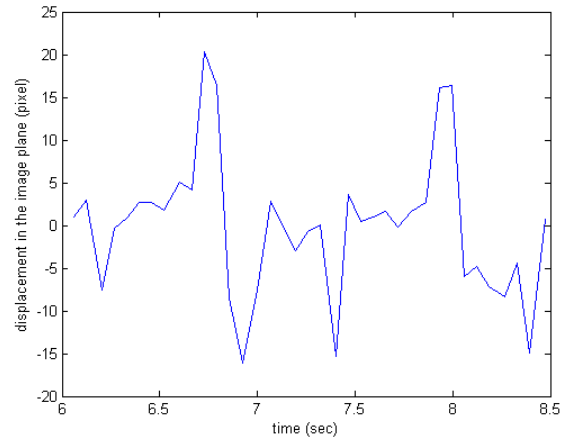


Fig. 7. Optical Flow Simulation for Fast Walking

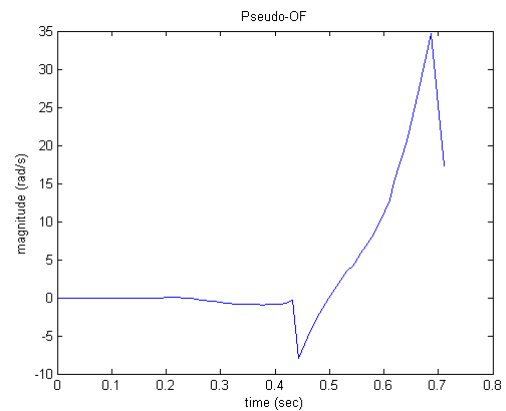


Fig. 8. Optical Flow Simulation for Fast Walking

These preliminary results suggest that OF sensors may provide useful information to support pedestrian navigation;

however, the specific motion models used in this paper may not be accurate enough to support high-precision navigation. One conclusion might be that a higher precision walking model, such as a passive walking model is needed. However, we hypothesize that it is also possible to improve our results significantly by refining our SLIP model. In particular, our current implementation of the SLIP model does not explicitly model double-stance, which occurs when both feet are simultaneously on the ground. During the double-stance phase, it would be most accurate to model the leg forces using two springs (rather than one as shown in Fig. 3). A refined kinematics model relating hip motion to shank motion might further improve the stride-length estimate. We will consider the impact of both model refinements in future work.

V. CONCLUSION

A means of estimating stride length using OF measurements is presented. The method relies on a simple dynamic model simulating human gait, specifically the Spring Loaded Inverted Pendulum (SLIP) model, which is a 2D motion model defined in the sagittal plane. The simulation allows an automated algorithm to predict values of OF data as a function of hip motion. By tuning model initial conditions (hip velocity at heel strike) and a control parameter (leg angle at heel strike), an optimization routine can identify the simulation that best matches measured OF data. That best-match simulation can then be used to estimate stride length.

An indoor test was performed to verify this algorithm and assess the quality of the SLIP model. In the trial, the algorithm correctly estimated stride length within 10%. This preliminary result suggests that model enhancements will be needed to extract higher accuracy stride-length estimates from the OF data. To this end, our future work will consider a refined SLIP model that accounts more accurately for double-stance and for shank kinematics.

REFERENCES

- [1] Garaj, V., "The Brunel Navigation System for Blind: Determination of the Appropriate Position to Mount External GPS Antenna on the User's Body," *Proceedings of the 14th International Technical Meeting of the Satellite Division of The Institute of Navigation (ION GPS 2001)*, Salt Lake City, UT, September 2001, pp. 274-279.
- [2] Makino, H., Ishii, I., Nakashizuka, M., "Development of navigation system for the blind using GPS and mobile phone combination," *Engineering in Medicine and Biology Society, 1996. Bridging Disciplines for Biomedicine. Proceedings of the 18th Annual International Conference of the IEEE*, vol.2, no., pp.506-507 vol.2, 31 Oct-3 Nov 1996.
- [3] Hsiao, C.C., Huang, P., "Two Practical Considerations of Beacon Deployment for Ultrasound-Based Indoor Localization Systems," *Sensor Networks, Ubiquitous and Trustworthy Computing, 2008. SUTC '08. IEEE. Conference on*, vol., no., pp.306-311, 11-13 June 2008.
- [4] Krishnan, S., Sharma, P., Zhang Guoping, Ong Hwee Woon, "A UWB based Localization System for Indoor Robot Navigation," *Ultra-Wideband, 2007. ICUWB 2007. IEEE International Conference on*, vol., no., pp.77-82, 24-26 Sept. 2007.
- [5] Biswas, J., Veloso, M., "WiFi localization and navigation for autonomous indoor mobile robots," *Robotics and Automation (ICRA), 2010 IEEE International Conference on*, vol., no., pp.4379-4384, 3-7 May 2010.

- [6] Foxlin, E., "Pedestrian tracking with shoe-mounted inertial sensors," *Computer Graphics and Applications, IEEE*, vol.25, no.6, pp.38-46, Nov.-Dec. 2005.
- [7] Jirawimut, R., Prakoornwit, S., Cecelja, F., Balachandran, W., "Visual odometer for pedestrian navigation," *Instrumentation and Measurement, IEEE Transactions on*, vol.52, no.4, pp. 1166- 1173, Aug. 2003.
- [8] Green, W.E., Oh, P.Y., Barrows, G., "Flying insect inspired vision for autonomous aerial robot maneuvers in near-earth environments," *Robotics and Automation, 2004. Proceedings. ICRA '04. 2004 IEEE International Conference on*, vol.3, no., pp. 2347- 2352 Vol.3, 26 April-1 May 2004.
- [9] Srinivasan, M.V., Zhang, S.W., Lehrer, M., Collett, T.S., "Honeybee Navigation en Route to the Goal: Visual Flight Control and Odometry," *The Journal of Experimental Biology* 199, pp. 237-244, 1996.
- [10] McGeer, T., "Passive Dynamic Walking," *The International Journal of Robotics Research* April 1990 vol. 9 no. 2 pp. 62-82
- [11] Srinivasan, M., Holmes P., "How well can spring-mass-like telescoping leg models fit multi-pedal sagittal-plane locomotion data?," *Journal of Theoretical Biology*, vol. 255, issue 1, 7 November 2008, pp. 1-7.
- [12] Barrows, G., "Mixed-Mode VLSI Optic Flow Sensors for Micro Air Vehicles," *Ph.D. Dissertation*, University of Maryland, College Park, MD, Dec. 1999.
- [13] Srinivasan, M. V., "An image-interpolation technique for the computation of optic flow and egomotion," *Biological Cybernetics*, vol. 71, issue 5, November 1994, pp. 401-415.
- [14] Horn, B. and Schunck, B., "Determining optical flow," *Artificial Intelligence*, vol. 17, issues 1-3, August 1981, pp. 185-203.
- [15] Beauchemin, S., Barron, J., "The computation of optical flow," *ACM Computing Surveys*, vol. 27, no. 3, pp. 433-467, 1995.
- [16] Matthews, C., Ketema, Y., Gebre-Egziabher, D., Schwartz, M., "In-situ step size estimation using a kinetic model of human gait," *Proc. ION GNSS 2010*, pp. 511-524, September 2010.
- [17] Full, R., Koditschek, D., Templates and anchors: neuromechanical hypotheses of legged locomotion on land, *Journal of Experimental Biology*, vol. 202, pp. 3325-3332, 1999.